ARTICLE
Journal of Cellular Biochemistry 113:2884–2894 (2012)

Journal of Cellular Biochemistry

Junctophilin 2 Knockdown Interfere With Mitochondrium Status in ESC-CMs and Cardiogenesis of ES Cells

Xingguang Liang,[1,2] Yuqin Mei,[1] Xin Huang,[3] Guofang Shen,[1] Danyan Zhu,[1] Yongping Yu,[4] Jianan Wang,[3*] and Yijia Lou[1**]

[1] *Division of Cardio-Cerebral Vascular and Hepatic Pharmacology, College of Pharmaceutical Sciences, Zhejiang University, Hangzhou 310058, China*

[2] *Department of Clinical Pharmacology, 1st Affiliated Hospital of Zhejiang University School of Medicine, Hangzhou 310003, China*

[3] *Cardiovascular Institute, Clinical Research Center, 2nd Affiliated Hospital at School of Medicine, Zhejiang University, Hangzhou 310009, China*

[4] *Institute of Materia Medica, College of Pharmaceutical Sciences, Zhejiang University, Hangzhou 310058, China*

ABSTRACT

In the present study, we explored the possible links between *Junctophilin 2* (*Jp2*) and the mitochondrium-sarcoplasmic reticulum (SR) interaction in embryonic stem cell-derived cardiomyocytes (ESC-CMs), as well as the role of *Jp2* in cardiogenesis of ES cells. We found that Ca^{2+} transient was abnormal and mitochondria were de-energized within si*Jp2* ESC-CMs. The essential juxtaposition structure of mitochondrium with SR was destroyed accompanied by selectively downregulation of *Pgc-1α*, *Nrf-1*, and *Mfn-2*. Impaired co-localization of the JP2 and sarcomeres (α-Actinin or Troponin-T) appeared in embryoid bodies (EBs) after *Jp2* knockdown. Calsequestrin2 and ryanodine receptor 2 within SR were expressed as early as the initiation of differentiation, while triadin and caveolin3 within t-tubules (TTs) did not appear until the terminal, indicating that JP2 probably did not contribute to anchoring the SR to TTs at the early cardiogenesis stage as usual. In addition, *Jp2* knockdown selectively decreased gene transcription toward cardiogenesis (*Brachyury*, *Isl1*, and *Nkx2.5*), subsequently weaken EB beating activity by 60%. Taken together, reducing JP2 expression in ESC-CMs resulted in impaired mitochondrial status due to either abnormal cellular Ca^{2+} homeostasis or disturbing of juxtaposition. A sensitive time window of JP2 necessary in cardiac differentiation was found at early stage via an extra non-TTs/SR anchor-dependent role. J. Cell. Biochem. 113: 2884–2894, 2012.

KEY WORDS: MITOCHONDRIUM-SR INTERACTIONS; JUNCTOPHILIN 2; CARDIOGENESIS; ESC-CMs; Ca^{2+} FLUX

Abbreviation used: $[Ca^{2+}]_i$, intracellular Ca^{2+} concentration; CICR, Ca^{2+}-induced Ca^{2+} release; CSQ2, calsequestrin2; cav3, caveolin3; ES cells, embryonic stem cells; EBs, embryoid bodies; ESC-CMs, ES cell-derived cardiomyocytes; EC, excitation-contraction; ER, endoplasmic reticulum; FCS, FACScan; GAPDH, glyceraldehyde-3-phosphate dehydrogenase; HF, heart failure; HCM, hypertrophic cardiomyopathy; JP2, Junctophilin 2; JMCs, junction membrane complexes; ΔΨm, Mitochondrial Membrane Potential; MEF, mouse embryonic fibroblasts; MEF2C, myocyte enhancer factor 2C; β-MHC, β-myosin heavy chain; PM, plasma membrane; RNAi, RNA interference; RyR2, ryanodine receptor 2; siRNA, small interfering RNA; si-ctr, scrambled small interfering RNA; SR, sarcoplasmic reticulum; TTs, transverse-tubules.

Additional supporting information may be found in the online version of this article.

Conflicts of interest: None.

Grant sponsor: National Natural Science Foundation of China; Grant numbers: 30973600, 90813026, 81173135; Grant sponsor: Ministry of Science and Technology of China; Grant number: 2009ZX09303-004; Grant sponsor: Outstanding Researcher Program in Medicine & Health Foundation of Zhejiang Province; Grant number: 2011RCA024.

*Correspondence to: Jianan Wang, MD, PhD, Cardiovascular Institute, Clinical Research Center, 2nd Affiliated Hospital at School of Medicine, Zhejiang University, Hangzhou 310009, China. E-mail: wang_jian_an@tom.com

**Correspondence to: Yijia Lou, PhD, Division of Cardio-Cerebral Vascular and Hepatic Pharmacology, College of Pharmaceutical Sciences, Zhejiang University, Hangzhou 310058, China. E-mail: yijialou@zju.edu.cn

Manuscript Received: 15 February 2012; Manuscript Accepted: 6 April 2012

Accepted manuscript online in Wiley Online Library (wileyonlinelibrary.com): 17 April 2012

DOI 10.1002/jcb.24164 • © 2012 Wiley Periodicals, Inc.

Cardiomyocytes are the cells with the highest volume density of mitochondrium for their extraordinary energy demand for continuous synthesis of ATP by oxidative metabolism. Mitochondrial number and functional capacity are dynamically regulated in accordance with energy demands and in response to diverse physiological conditions, including Ca^{2+} homeostasis. Mitochondria are located within 20 nm of the sarcoplasmic reticulum (SR) and thereby exposed to a high local $[Ca^{2+}]_i$ during the Ca^{2+} release process, the mitochondrium and SR Ca^{2+} cycling is of vital importance to cardiac cell function and plays an important role in embryonic development [Rizzuto and Pozzan, 2006; Lukyanenko et al., 2009], thus, the close contact of mitochondrium-SR is crucial for mitochondrial biological function.

It was reported that mitofusin 2 (Mfn2), which was enriched at the contact sites between mitochondrium and SR, bridged the mitochondrium to SR by engaging in homotypic and heterotypic complexes with Mfn1, and formed a juxtaposition required for efficient mitochondrial Ca^{2+} uptake [Eura et al., 2006; de Brito and Scorrano, 2008]. Silencing of *Mfn2* in mouse embryonic fibroblasts disrupted SR morphology and loosened mitochondrium-SR interaction, thereby reducing the efficiency of mitochondrial function [Chen et al., 2003]. More and more evidence indicated that the juxtaposition between mitochondrium and SR provided a physical basis for intercommunication during Ca^{2+} signaling and endowed with key players of the Ca^{2+}-handling machinery [de Brito and Scorrano, 2008; de Brito and Scorrano, 2009; Parekh, 2009].

Junctophilin 2 (JP2), a unique subtype rich in the heart, is essential for cellular Ca^{2+} homeostasis and cardiac excitation-contraction (EC) coupling [Takeshima et al., 2000; Minamisawa et al., 2004]. It had been demonstrated that cardiomyocytes from the mutant mice lacking JP2 showed deficiency of the junctional membrane complexes (JMCs) and abnormal Ca^{2+} transients, leading to embryonic lethality [Takeshima et al., 2000]. Moreover, mutation of *Jp2* genes was closely associated with hypertrophic and dilated cardiomyopathies such as heart failure (HF), which was characterized by reduction of contractile function and defects in Ca^{2+} handling in cardiomyocytes [Takeshima, 2003; Landstrom et al., 2007; Kee and Kook, 2009; Woo et al., 2010].

Ca^{2+} signaling is of vital importance to cardiac cell function and plays an important role in HF, based on SR and mitochondrium Ca^{2+} cycling. The requirement for steady-state Ca^{2+} flux balance applies not only to SR Ca^{2+} cycling, but also for Ca^{2+} entry and exit on the mitochondrium, however, so far the role of JP2 on mitochondrium status has not been investigated yet. Here we hypothesized that abnormal Ca^{2+} transients in cardiomyocytes might induce deficiency of functional crosstalk between mitochondrium and SR. We therefore employed a siRNA-based interference approach to exploring the influence of *Jp2* knockdown on the mitochondrium statues and mitochondrium-SR juxtaposition in embryonic stem cell-derived cardiomyocytes (ESC-CMs).

In addition, despite progress in JP2, little is known about its roles in differentiated progeny from ES cells. In present study, we try to explore whether or not a sensitive time window of *Jp2* gene expression existed in cardiac differentiation. We also try to characterize the crucial Ca^{2+} handling proteins which link the developing organization of proteins with JP2 underlying EC coupling in cardiogenesis of ES cells or ESC-CMs.

MATERIALS AND METHODS

CELL CULTURE AND CARDIOMYOCYTE DIFFERENTIATION

Mouse ES cell D3 (CRL-1934, American Type Culture Collection, Manassas, VA) were cultured in DMEM medium (Gibco, Grand Island, NY) supplemented with 1% nonessential amino acids (NEAA, Gibco), 10% fetal bovine serum (FBS, Gibco), 0.1 mmol/L β-mercaptoethanol (Sigma-Aldrich, St. Louis), and 10^6 units/L mouse leukemia inhibitory factor (Chemicon, CA)-conditioned medium in a humidified 5% CO_2 atmosphere at 37°C. Embryoid bodies (EBs) were formed by hanging drop method in EB medium (DMEM with 20% FBS, 0.1 mmol/L β-mercaptoethanol, and 1% NEAA). After 3 days of differentiation in hanging drop and 2 days of suspension culture, EBs were placed on gelatin (0.1%, Sigma)-coated 24-well plates in differentiation medium [Metzger et al., 1996]. Daily microscopic observations were conducted to detect beating EBs and determine the beating rate [Wobus et al., 1997; Boheler et al., 2002; Ding et al., 2008; Wo et al., 2008b].

ISOLATION OF ESC-CMS

The spontaneously contracting EBs were detached from culture surfaces by incubating with 0.05% trypsin-EDTA for 1 min at 37°C, then dispersed into cells with 1 g/L collagenase (CLSII, Worthington Biochemical) for 30 min at 37°C. After digesting into separated cells, ESC-CMs were isolated by centrifugation at 1,500*g* for 30 min through a discontinuous Percoll (GE Healthcare Life Sciences) gradient (40.5 and 58.5%) and collected at the interface of the two layers. After removal of the top layer, ESC-CMs were collected and washed twice in PBS and adhered onto glass coverslip coated with 1% gelatin.

TARGETED SIRNA TRANSFECTION AGAINST JP2

RNA interference (RNAi) the small-interference (si) RNAs were targeted si*Jp2* into either ES cells or ESC-CMs. siRNA targeting mouse JP2 mRNA as well as a validated negative control siRNA labeled with the Alexa-488 dye were ordered from Qiagen (Valencia, CA). Target si*Jp2*-a sequence: CCGCCACAATGTGCTGGTCAA, si*Jp2*-b: CTGTATGGTGATCTTGCTGAA. Briefly, siRNA-negative-control, si*Jp2* (200 pmol) were complexed with 2 μl of lipofectamine2000 (Invitrogen) in a final volume of 200 μl Opti-MEM medium. The complexes were added onto freshly passaged ES cells or 17days old ESC-CMs (150,000 cells/well). Twenty four hours after transfection, cells were harvested for EB formation or further measurements [Li et al., 2006].

ANALYSIS OF ESC-CMS CELL SIZE

After incubation in si*Jp2* medium for 48 h, the cells were washed in PBS and fixed in 4% formaldehyde, subsequently permeabilization with 0.1% Triton X-100, the fixed cells were then incubated in 1% bovine serum albumin (BSA) for 30 min. For cell size measurement, cells were incubated for 3 h at room temperature with FITC-conjugated Phalloidin (1:300; Molecular Probes, Eugene, OR). Cell images were taken under a Leica fluorescence microscope.

Ca^{2+} TRANSIENT MEASUREMENT

A spectrofluorometric method with Fluo-4/AM as the Ca^{2+} indicator was used for measuring $[Ca^{2+}]_i$. ESC-CMs transfected with si-ctr or si*Jp2* for 24 h were rinsed with bath solution (mmol/L): 140 NaCl, 5 KCl, 1 $CaCl_2$, 1 $MgCl_2$, 10 glucose, and 10 HEPES, incubated in bath solution containing 5 μmol/L Fluo-4/AM and 0.02% Pluronic F-127 with 5% CO_2, 95% O_2 at 37°C for 30 min. The temporal resolution of the line scan was 439 Hz. Ten millimoles per liter caffeine and 8 mmol/L $CaCl_2$ were added as stimulator. A cooled CCD camera mounted on the microscope equipped with a polychromator (IX S1, Olympus) was used to capture the fluorescence data with excitation at 488 nm and emission at 510 nm at room temperature [Hirata et al., 2006; Kapur and Banach, 2007; Satin et al., 2008]. All analyses of $[Ca^{2+}]_i$ were processed at a single-cell level and expressed as the relative fluorescence intensity.

MITOCHONDRIAL MEMBRANE POTENTIAL ($\Delta\Psi$M) ASSESSMENT

JC-1 staining was used to assess the mitochondrial $\Delta\Psi$m in si*Jp2* ESC-CMs. JC-1 exhibited potential-dependent accumulation in mitochondrium, indicated by a fluorescence emission shift from green (525 ± 10 nm) to red (610 ± 10 nm). Mitochondrium depolarization was specifically indicated by a decrease in the red to green fluorescence intensity ratio [Zuliani et al., 2003].

TRANSMISSION ELECTRON MICROSCOPE

Structures of the mitochondrium and SR in ESC-CMs were analyzed by transmission electron microscope. The cells were fixed with 2.5% glutaraldehyde in 0.1 mol/L phosphate buffer for 2 h at 4°C, followed by postfixation in aqueous 1% osmium tetroxide for 1 h at 4°C. The samples were then dehydrated in graded acetones, permeated, and embeded in Polybed 812 epoxy resin (Polysciences). Ultrathin sections (approximately 75 nm) were prepared and stained with 2% uranyl acetate, followed by 1% lead citrate. Sections were photographed under a transmission electron microscope.

REVERSE TRANSCRIPTION–POLYMERASE CHAIN REACTION (RT–PCR)

Total RNA was isolated from EBs using Trizol reagent (Gibco) in accordance with the manufacturer's instructions. To synthesize first strand cDNA, 3 mg total RNA was incubated with 0.5 mg of oligo (dT) (Sangon, China) and 5 ml deionized water at 65°C for 15 min. Reverse transcription reactions were performed with 200 units of M-MuLV reverse transcriptase (Gibco), 4 ml of 5 μmol/L reaction buffer and 1 mmol/L deoxynucleoside triphosphate (dNTP) mixture for 1 h at 42°C. Polymerase chain reactions of 50 ml contained 1 ml of the RT reaction product, 5 ml of 10 μmol/L PCR buffer, 25 units Taq polymerase, 1 ml of 10 mmol/L dNTP mixture, and 30 pmol of each primer (Sangon). Primers, annealing temperature, product size, and number of PCR cycles were depicted in Table I. The PCR products were analyzed by 1.5% agarose (Biowest, Spain) gel electrophoresis, visualized with ethidium bromide staining, and then quantified using a bio-imaging analyzer (Bio-Rad). The density of the products was quantified using Quantity One version 4.2.2 software (Bio-Rad). *GAPDH* was used as an internal standard. mRNA from three independent experiments were analyzed [Ding et al., 2007c].

WESTERN BLOT ANALYSIS

Cells were collected in RIPA buffer (containing 0.2% Triton X-100, 5 mmol/L EDTA, 1 mmol/L PMSF, 10 μg/ml leupeptin, 10 μg/ml aprotinin, added with 100 mmol/L NaF, and 2 mmol/L Na_3VO_4) and

TABLE I. Sequence for the Primers and Conditions of PCR

Gene	Primer sequence (5′–3′)	Annealing temperature (°C)	Product size (bp)	Cycle
JP-2	Forward: GCCGCTTTGACTTTGATGAT Reverse: TCCGTCTGCGTAGGTCTCC	58	196	45
Oct-4	Forward: AGGGATGGCATACTGTGGAC Reverse: CCTGGGAAAGGTGTCCTGTA	60	73	35
Fgf-5	Forward: CAGAGTGGGCATCGGTTTC Reverse: CTTCACTGGGCTGGGACTT	58	466	35
Branchy	Forward:TGCTGCCTGTGAGTCATAAC Reverse:AAGGGAGGACATTAGAGGTG	65	726	35
Afp	Forward: CCATGTACATGAGCACTGTTG Reverse: CTCCAATAACTCCTGGTATCC	57	300	35
Nkx-2.5	Forward: CAAGTGCTCTCCTGCTTTCC Reverse: GGCTTTGTCCAGCTCCACT	54	136	35
Isl-1	Forward: GTT TGTACGGGA TCA AATGC Reverse: ATG CTG CGT TTC TTG TCCTT	60	503	35
MEF-2C	Forward: GATACCCACAACACACCACGCGC Reverse: ATCCTTCAGAGAGTCGCATGCGCTT	60	197	38
GATA-4	Forward: TCTCACTATGGGCACAGCAG Reverse: GCGATGTCTGAGTGACAGGA	54	135	33
β-MHC	Forward: CTGCTGGAGAGGTTATTCCTCG Reverse: GGAAGAGTGAGCGGCGCATCAAGG	66	301	38
Pgc-1α	Forward: AGAAGCGGGAGTCTGAAA Reverse: CACAGGTGTAACGGTAGG	58	216	35
Nrf-1	Forward: ATCCAGACGACGCAAGCA Reverse: TGGTGACAGTGGCTCCCT	56	103	35
Mfn-1	Forward: TCATTCTGAATAACCGTTGG Reverse: TCACTGCTGACTGCGAGA	53	303	35
Mfn-2	Forward: AAGTCCGGGAAGCTGAAAGT Reverse: TCTCGGTTATGGAACCAACC	58	160	35
GAPDH	Forward: AACTTTGGCATTGTGGAAGG Reverse: ACACATTGGGGGTAGGAACA	58	223	25

lysed 30 min on ice. Protein concentration was assayed using the Bio-Rad protein kit (Hercules, CA), and equal amounts of sample were loaded per well on a sodium dodecyl sulphate (SDS)-polyacrylamide gel. Subsequently, proteins were transferred onto 0.45 μm pore size positively charged nylon membranes (PVDF, Millipore) and blocked with blotto (5% dry milk in PBS with 0.1% Tween-20) at room temperature. The blots were challenged with primary antibody in blotto overnight at 4°C, followed by washing three times with PBST (0.1% Tween-20), and challenged with HRP-conjugated goat anti-rabbit, rabbit anti-goat, or mouse anti-mouse antibodies, respectively, followed by detection with an enhanced chemiluminescent substrate (ECL, Pierce, Rockford, IL). As primary antibodies, the mouse monoclonal anti-Troponin T (Santa Cruz) or anti-α-Actinin (Sigma) or rabbit polyclonal anti-JP2 (Invitrogen) or anti-RyR2 (Santa Cruz) or goat polyclonal anti-triadin (Santa Cruz) or anti-CSQ2 (Santa Cruz) or anti-cav3 (Santa Cruz) were used [Ding et al., 2007a].

IMMUNOCYTOCHEMISTRY ANALYSIS

Immunofluorescence was performed with whole outgrown EBs. EBs were fixed with methanol at −20°C for 15 min, followed by permeabilization in 0.1% Tween-20, then were blocked with 10% FBS for 30 min at room temperature and incubated in PBS containing mouse monoclonal anti-Troponin T (Santa Cruz) or anti-α-Actinin (Sigma) or rabbit polyclonal anti-JP2 (Invitrogen) or goat polyclonal anti-triadin (Santa Cruz) or anti-calsequestrin2 (Santa Cruz) or anti-cav3 (Santa Cruz), rabbit polyclonal anti-RyR2 (Santa Cruz) overnight at 4°C, EBs were washed in PBS three times, followed by incubation in blocking buffer containing Alexa fluor 488-conjugated anti-mouse IgG (Invitrogen) or Alexa fluor 594-conjugated anti-rabbit IgG (Invitrogen) or Alexa fluor 594-conjugated anti-goat IgG (Invitrogen). Fluorescence image was performed by fluorescence inverted microscope [Muller et al., 2000; Ding et al., 2008].

FLOW CYTOMETRY ANALYSIS

EBs obtained at day 17 of differentiation were dissociated to a single-cell suspension by 0.25% trypsin-EDTA treatment. For intracellular staining, cells were fixed with 4% paraformaldehyde for 1 h and then treated with 10% FBS to block non-specificantigens. EBs were incubated in PBS containing mouse monoclonal anti-Troponin T (Santa Cruz) or anti-α-Actinin (Sigma) or rabbit polyclonal anti-JP2 (Invitrogen) overnight at 4°C. After rinsing in washing buffer, cells were incubated with Alexa fluor 488-conjugated anti-mouse IgG (Invitrogen) or phycoerythrin-conjugated anti-rabbit IgG (Invitrogen) for 1 h, and then suspended in 0.5 ml 1% BSA and analyzed on a FACScan (Becton Dickinson, Heidelberg). The fluorochrome was detected at 530 nm in the FL-1 and FL-2 channel. Each plot represented 10,000 viable cells (non-viable cells were excluded from FACS analysis by appropriate gating). Untreated cells and cells lacking primary antibody were used as negative controls. In addition, isotype controls were used to assess the level of non-specific antibody binding. All data analyses were carried out using CellQuest software (Becton Dickinson) [Muller et al., 2000; Li et al., 2005].

STATISTICAL ANALYSIS

OriginLab and GraphPad InStat software were used for statistical analyses. Values are expressed as means ± SD. Student's *t*-test was used for comparing paired and unpaired data from two populations, and one-way analysis of variance (ANOVA) used for multiple group comparisons. The value $P < 0.05$ was considered statistically significant.

RESULTS

siJP2 INFLUENCED INTACT MITOCHONDRIUM AND SR IN ESC-CMS

To explore whether knockdown of *Jp2* expression by acute siRNA in purified ESC-CMs resulted in mitochondrial dysfunction, we evaluated the mitochondrial ΔΨm, ultrastructure and the gene expressions related the mitochondrium-SR interactions. We found that si*Jp2* resulted in a shift toward low ΔΨm after 2 h transient transfection (green) compared with that of si-ctr cells (red/orange), and was reduced more than 60% in si*Jp2* ESC-CMs (Fig. 1A). This indicated that the mitochondrium of si*Jp2* ESC-CMs were de-energized, which could be caused by mitochondrial electron transport chain uncoupled from ATP production [Behbahani et al., 2006]. Data we present here were the first evidence showing that *Jp2* knockdown in ESC-CMs affects physiological functions of energy production.

Ultrastructures of the rough SR and mitochondrium were further analyzed in ESC-CMs. Compared to si-ctr cells, the cord-like rough SR embeded around the mitochondrium disappeared in si*Jp2* cells, suggesting that *Jp2* knockdown produced damage on the intracellular organelles, e.g., swollen mitochondrium with degraded cristae (Fig. 1B right), fragmented rough SR elements (Fig. 1B right, arrowhead). Based on the evidences, we believed that the necessary juxtaposition of the SR with mitochondrium is destroyed followed by blocking Ca^{2+} fluxes between the organelles.

Furthermore, we found that si*Jp2* reduced the expression of peroxisome proliferator-activated receptor γ coactivator-1α gene *Pgc-1α*, transcription factor regulating oxidative phosphorylation enzyme gene *Nrf-1* and GTP-dependent mitochondrial fusion gene *Mfn-2* after 48 h transient transfection, while expression of *Mfn-1* was up-regulated (Fig. 1C), suggesting that the mitochondrial function and mitochondrium-SR interactions were influenced by acute si*Jp2*. The responsive gene expression might contribute to the mechanisms in mitochondrial dysfunction and juxtaposition of mitochondrium with SR.

REDUCED MEF-2C TRANSCRIPTION AND DISRUPTED Ca^{2+} TRANSIENTS IN siJP2 ESC-CMs

si*Jp2* in purified ESC-CMs resulted in JP2 sharp down-expression (Fig. 2A). Notably, there was only Ca^{2+} related hypertrophic markers gene *MEF-2C* transcription increased by 20% in si*Jp2* ESC-CMs after 48 h transient transfection, while little changed in expression of other known markers of cardiac hypertrophy, such as *GATA4*, *β-MHC* (Fig. 2B).

Whether *Jp2* knockdown affected Ca^{2+} transients was further evaluated in either spontaneously beating or non-beating ESC-CMs. To evaluate total SR $[Ca^{2+}]_i$, we measured the peak of RyR agonist caffeine-induced $[Ca^{2+}]_i$ transients. Representative tracing showed

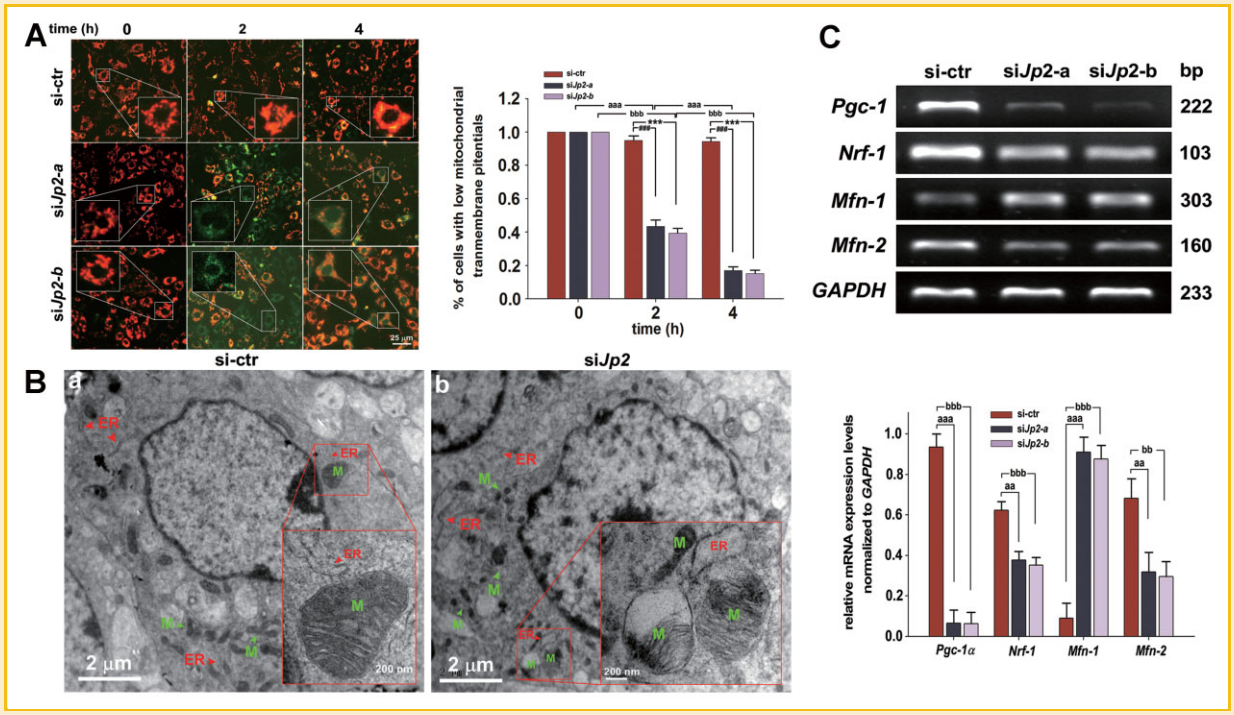

Fig. 1. Knockdown of JP2 expression by acute siRNA in purified ESC-CMs caused mitochondria injury and abnormal mitochondrial related genes expression. A: Mitochondrial membrane potential ($\Delta\Psi m$) assessment of ESC-CMs by JC-1 staining. ESC-CMs were treated with si*Jp2* followed by JC-1 staining. Mitochondrial $\Delta\Psi m$ was specifically indicated by a decrease in the red to green fluorescence intensity ratio (reduced more than 60% in si*Jp2* ESC-CMs). Scale bar = 25 μm. B: Ultrastructures of the rough SR and mitochondria were analyzed in ESC-CMs. (a) In the si-ctr cell, cord-like rough SR (arrowhead) embedded around the mitochondrium (M). (b) In the si*Jp2* cell, cord-like rough SR disappeared, replacing with fragmented SR elements (arrowhead) and mitochondria showed swollen structures with degraded cristae. Scale bar = 2 μm. C: Effects of si*Jp2* on mRNA expression of mitochondrial related genes. si*Jp2* cells reduced the expression of peroxisome proliferator-activated receptor γ coactivator-1α gene *Pgc-1α*, transcription factor regulating oxidative phosphorylation enzyme gene *Nrf-1* and ATP-dependent mitochondrial fusion gene *Mfn-2* after 48 h transient transfection, while expression of *Mfn-1* was up-regulated. [Color figure can be seen in the online version of this article, available at http://wileyonlinelibrary.com/journal/jcb]

that there was a change in SR Ca^{2+} content stability between si-ctr and si*Jp2* beating cells, indicated by several lower and disorderly amplitudes after transients in si*Jp2* cells. Caffeine-evoked $[Ca^{2+}]_i$ transients recorded in si-ctr non-beating ESC-CMs appeared with a sharp peak, suggesting that the ability of the SR Ca^{2+} storage still kept normal. In contrast, the same ability almost disappeared in si*Jp2* ESC-CMs (Fig. 2C, upper). The relationship between L-type calcium current (ICa) and $[Ca^{2+}]_i$ by Ca^{2+}-induced Ca^{2+} release (CICR) kept almost normal rhythm in si-ctr beating ESC-CMs, but disappeared in si*Jp2* group. Similarly, there was a change in CICR between si-ctr and si*Jp2* non-beating ESC-CMs, indicated by a single peak in si-ctr cell and several disorderly amplitudes after transients in si*Jp2* cell (Fig. 2C, down).

CHARACTERIZATIONS OF JP2 IN CARDIOGENESIS OF ES CELLS

Beating phenotype was evaluated during cultivation from day 8 up to 17 after EBs plating (Fig. 3A). JP2 expression was analyzed by RT-PCR or western blot during the differentiation course (Fig. 3B1). The result showed that both JP2 protein expression and beating EBs percentage increased in a time-dependent manner from day 9 to 17. Immunofluorescence microscopy was employed to reveal the distribution of JP2, probing for merging of JP2 and sarcomeric α-Actinin or Troponin-T in small clusters. The result showed a well matched co-localization of JP2 with the cardiac proteins on day 17 (Fig. 3C). Furthermore, cells double-staining with JP2 and Troponin-T or α-Actinin were analyzed quantitatively by FCS analysis on day 17. The results showed that $8.23 \pm 3.01\%$ of cells stained positive for Troponin-T and JP2, and $12.16 \pm 1.86\%$ for α-Actinin and JP2, respectively (Fig. 3 B2), which was very close to the data in spontaneously cardiac differentiation in our previous research [Ding et al., 2008; Wo et al., 2008a].

EXPRESSION AND LOCALIZATION OF Ca^{2+}-HANDLING PROTEIN COMPONENTS WITHIN EBS

The co-expression of triadin, RyR2, cav3, and CSQ2 with sarcomeric α-Actinin or Troponin-T was evaluated in ESC-CMs. Co-localization of all the proteins in sarcomeric structures were showed on day 17 (Fig. 3C). The results demonstrated that they occupied the appropriate sites together with JP2 within maturing structures in synchrony. The overall expression of proteins linking the developing organization was also analyzed in EBs. Interestingly, the expression of CSQ2 and RyR2 appeared as early as beginning of the differentiation and increased in a time-dependent manner. As to triadin and cav3, surprisingly, they did not appear until the end of differentiation (day 13–17) (Fig. 3D). It meant that JP2, together with RyR2, a definite protein marker for SR, and cav3, a marker for

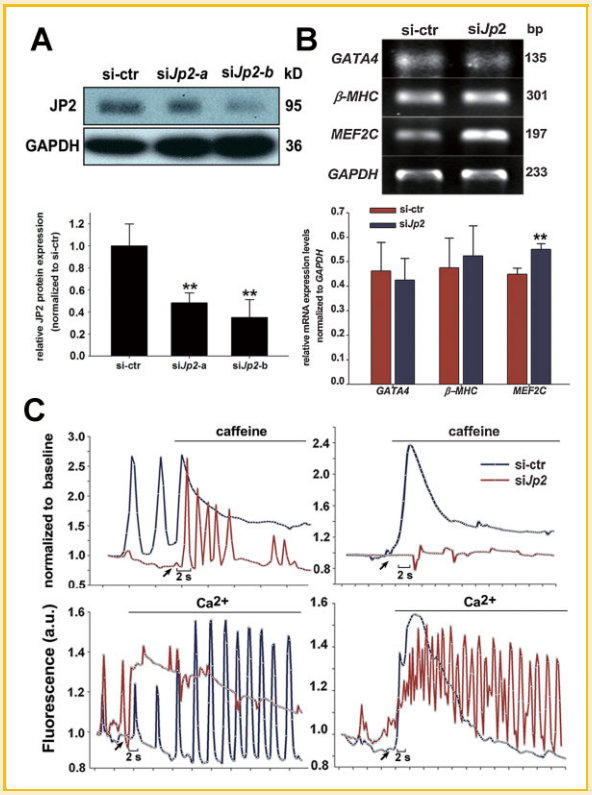

Fig. 2. Knockdown of JP2 expression by acute siRNA in purified ESC-CMs altered Ca^{2+} flux and store Ca^{2+} levels. A: Western blot analysis showed that the expression of JP2 was strongly decreased in *Jp2*-knockdown ESC-CMs. Densitometric quantification of western blot against the indicated proteins, value was corrected with GAPDH band intensity as a loading correction. $^{**}P < 0.01$ versus si-ctr. B: Representative fluorescence recordings of caffeine-evoked Ca^{2+} transients or Ca^{2+}-induced Ca^{2+} transients. Whole cell Ca^{2+} transient was recorded with a cooled CCD camera mounted on the microscope imaging using freshly isolated ESC-CMs loaded with fluo-4 AM. The temporal resolution of the line scan was a profile of total fluorescence (arbitrary units) (left panel: Spontaneously beating ESC-CMs, right panel: Non-beating ESC-CMs). A total of 10 mmol/L caffeine and 8 mmol/L Ca^{2+} was added to the subpopulation of ESC-CM, respectively, ($n = 65$) in Ca^{2+}-free medium (indicated by an arrow). C: Expression of "hypertrophic" genes *GATA4*, *β-MHC*, and *MEF2C* was evaluated by semi-quantitative RT-PCR after 48 h si*Jp2* transfection of ESC-CMs. Only was up-regulation of *MEF2C* in the cells seen. Data were represented as means ± SD of three independent experiments. Statistic significance was set as $^{**}P < 0.01$ versus si-ctr. [Color figure can be seen in the online version of this article, available at http://wileyonlinelibrary.com/journal/jcb]

t-tubules (TTs), sheared the terminal cisternae assembled from at least two distinct membrane components in ESC-CMs. It suggested that at the early developmental stages of cardiogenesis (day 5–9), JP2 probably did not take a role in anchoring the SR to TTs.

DIFFERENTIATION TOWARD CARDIOGENESIS DISRUPTED IN siJP2 ES CELLS

siRNA was targeted *Jp2* into either ES cells or the progeny to investigate whether *Jp2* deficiency had an impact on cardiogenesis. The effect of si*Jp2* on beating phenotype was evaluated on day 17. Notably, the percentage of spontaneously contracting EBs and number of beating area were reduced by more than 60% in si*Jp2* EBs (Fig. 4A). It suggested that reduced *Jp2* expression in ES cells markedly prevented cardiac differentiation indicated by beating phenotype.

To verify whether this decrease also had an impact on myofibrillogenesis, we evaluated the organization of the sarcomeric proteins in EBs. As shown in Figure 4B, there was co-localization of JP2 with either α-Actinin or Troponin-T sarcomeric structures on day 9 or 17 cardiomyocytes differentiated from si-ctr ES cells, respectively. In contrast, cardiomyocytes derived from si*Jp2* ES cells showed a JP2 down-expression accompanied by disorderly sarcomeric structure for α-Actinin and no interconnected network of myofibrils for Troponin-T. Taken together, decreased *Jp2* expression did have an effect on sarcomeric protein expression followed by abnormal sarcomere formation in cardiomyocytes.

Based on above findings, we further investigated whether or not *Jp2* deficiency in ES cells had an impact on blastodermic layer development and consequently, on the expression levels of transcription factors known to be involved in cardiogenesis. Transcription of the pluripotency marker gene *Oct-4*, epiblast gene *Fgf-5*, mesoderm gene *Brachyury*, endoderm gene *Afp*, pre-cardiac mesoderm gene *Isl-1*, and cardiac progenitor cell gene *Nkx-2.5* were analyzed during early cardiac differentiation. Differentiation toward mesoderm and cardiogenesis was typically determined by the transcription of *Brachyury*, *Isl-1*, and *Nkx-2.5*. When compared with si-ctr EBs, *Jp2* knockdown group showed selectively decreased *Brachyury* (day 0–8), *Isl-1* (day 2–8), and *Nkx-2.5* (day 4–8) transcription during the early differentiation stage. *Oct-4* diminishing started from day 4, which meant that reduced *Jp2* transcription did not influence ES cell differentiation. *Fgf-5* showed no reduction in the process of si*Jp2* ES cell cardiac differentiation compared with that in si-ctr cells (Fig. 4C). Therefore, a sensitive time window of *Jp2* necessary in the early cardiac differentiation was found.

DISCUSSION

JP2 is a membrane-binding protein that plays a key role in the organization of the JMCs and maintenance of Ca^{2+} homeostasis [Takeshima et al., 2000; Minamisawa et al., 2004; Matsushita et al., 2007]. In cardiac myocytes, mitochondrium and SR Ca^{2+} cycling is also of vital importance to cardiac cell function and embryonic development [Rizzuto and Pozzan, 2006; Lukyanenko et al., 2009]. Thus, it is important to highlight the importance of JP2 related mitochondrium-SR relationship in cardiac physiology.

In this study, we first employed a siRNA-based interference *Jp2* to investigate the effects of decreased JP2 on the mitochondrium statue and mitochondrium-SR interaction in ESC-CMs. It was well known that the normal mitochondrial function was partly driven by the mitochondrial $\Delta\Psi m$. Maintenance of $\Delta\Psi m$ was fundamental for the normal performance and survival of cardiomyocytes which have a high-energy requirement [Wallace, 1999]. We found that a low mitochondrial $\Delta\Psi m$ specifically appeared in si*Jp2* ESC-CMs at early stage. This indicated the de-energized statue of mitochondrium caused by mitochondrial electron transport chain uncoupled from ATP production [Behbahani et al., 2006]. Most studies implicated

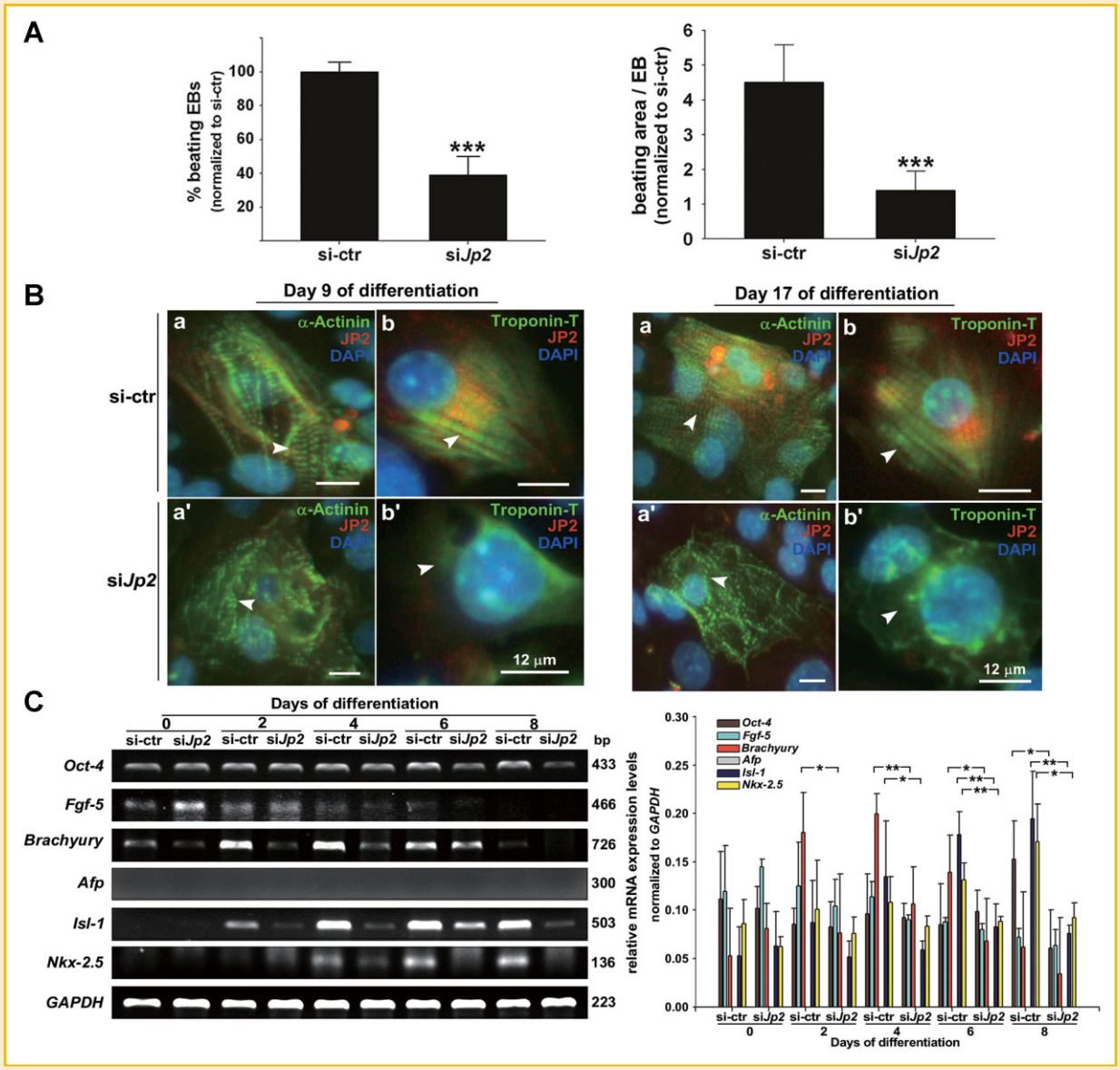

Fig. 3. Knockdown of JP2 expression by siRNA in ES cells impaired beating function and sarcomeric protein expression in ESC-CMs as well as gene expression towards mesoderm and cardiogenesis. A: Beating phenotype was evaluated on day 17 after EBs plating. *Jp2* knockdown decreased either beating rate or number of beating area in EBs. $^{***}P < 0.001$ versus si-ctr. Identical results were obtained from three independent experiments. B: Immunocytochemistry showed co-localizations (orange) of α-Actinin (a) or Troponin-T (b) sarcomeric structures (green, arrow) with JP2 (red) in day 9 or day 17 ESC-CMs. Abnormal sarcomeric structures accompanied by little JP2 expression in *Jp2* knockdown cells (a', b'). Nuclei were stained with DAPI (blue). C: Expressions of the pluripotency marker gene *Oct-4*, epiblast gene *Fgf-5*, mesoderm gene *Brachyury*, endoderm gene *Afp*, pre-cardiac mesoderm gene *Isl-1*, and cardiac progenitor cell gene *Nkx-2.5* were analyzed during early cardiac differentiation by semi-quantitative RT-PCR. *GAPDH* was used as a control. Differentiation towards mesoderm and cardiogenesis was determined by expression of *Brachyury, Isl-1, and Nkx-2.5*. *Jp2* knockdown selectively decreased *Brachyury, Isl-1 and Nkx-2.5* expression. A *Jp2* gene necessary sensitive time window (day 2–4) during cardiac differentiation was demonstrated. *Jp2* gene controlled the differentiation of ESCs into cardiac muscle, as well as mesoderm at early stage. $^{*}P < 0.05$, $^{**}P < 0.01$ versus si-ctr. Identical results were obtained from three independent experiments. [Color figure can be seen in the online version of this article, available at http://wileyonlinelibrary.com/journal/jcb]

that *Pgc-1α* was essential for the cardiac adaptive energy metabolic and triggered the coordinate activation of nuclear and mitochondrial genes *Nrf-1* which could drive mitochondrial biogenesis [Ding et al., 2007b; Shao et al., 2010]. It was also reported that mitochondrial biogenesis involved a Ca^{2+}-dependent pathway [Mercy et al., 2005]. Thus, together with decreased *Pgc-1α* and Nrf-1 transcription in the present study, we considered that low $\Delta\Psi m$ caused by si*Jp2* could be an early event in mitochondrial Ca^{2+} influenced energy production in si*Jp2* ESC-CMs, which might further impact the mitochondrial energy metabolic and juxtaposition of the mitochondrium and SR.

de Brito and Scorrano [2008, 2009] had found that the dynamin-related protein Mfn2 tethered the mitochondrium to SR, and juxtaposition of the mitochondrium and SR provided a privileged pathway for shuttling Ca^{2+} between them in a manner that obviated a more general and hence less specific bulk cytoplasmic Ca^{2+} rise.

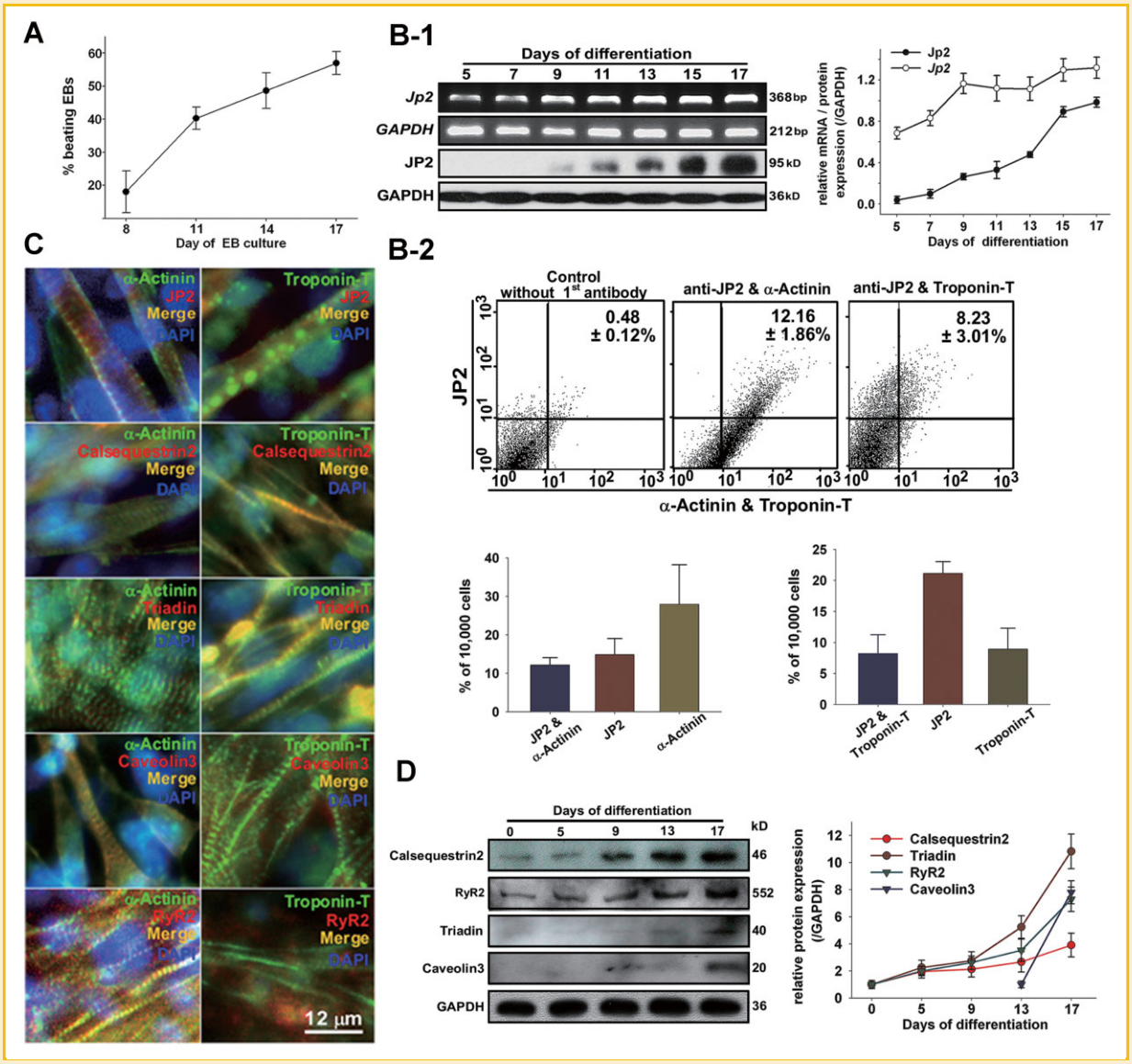

Fig. 4. Molecular and functional characterizations of JP2 and Ca^{2+}-handling proteins during the cardiac differentiation of ES cells. A: Beating phenotype was evaluated during cultivation from day 8 up to 17 after EBs plating. B-1: JP2 expression was analyzed by semi-quantitative RT-PCR and western blot during the course. B-2: JP2 and sarcomere proteins co-expression was quantified by flow cytometry within day 17 EBs. C: Immunocytochemistry showed the co-localization (orange) of sarcomere proteins (green, left: α-Actinin, right: Troponin-T) with JP2, calsequestrin2, triadin, caveolin3 and RyR2 (red) in day 17 ESC-CMs, respectively. Nuclei were stained with DAPI. Scale bar = 12 mm. D: Development-dependent expressions of calsequestrin2, triadin, caveolin3 and RyR2 were analyzed by western blot during the course. Data were represented as means ± SD of three independent experiments. [Color figure can be seen in the online version of this article, available at http://wileyonlinelibrary.com/journal/jcb]

Therefore, our finding further revealed that loss of JP2 markedly disrupted the juxtaposition of mitochondrium with SR, indicated by acutely reducing *Mfn2* transcription followed with the abnormal ultrastructure of mitochondrium and SR, for example, swollen mitochondrium with degraded cristae, fragmented rough SR elements. Ultrastructural defects of intracellular organelles further suggested the mitochondrial dysfunction which might cause energy depletion and the disruption of Ca^{2+} homeostasis in si*Jp2* cardiomyocytes.

It had been demonstrated that mitochondrial Ca^{2+} transport played a key role in the regulation of cardiac cell function [Rizzuto and Pozzan, 2006; Lukyanenko et al., 2009]. The mitochondrial Ca^{2+} uptake from SR was crucial for mitochondrial physiological function. Here we found that reduced *Jp2* expression led to abnormal RyR2 activation and CICR. The peak amplitude of Ca^{2+} current through the cav3 in whole-cell Ca^{2+} transient by CICR disappeared after si*Jp2*, which suggested that JP2 selectively disrupted the link between L-type calcium current (ICa) and $[Ca^{2+}]_i$. Caffeine-evoked $[Ca^{2+}]_i$ transients in si-ctr ESC-CMs appeared with a sharp peak, suggesting that the ability of the SR Ca^{2+} storage still kept normal, while the same ability almost disappeared in si*Jp2* ESC-CMs. This was similar with the result of a recently research about JP2 expression knockdown could cause abnormal intracellular calcium-handling in mouse atrial cardiomyocytes tumor lineage

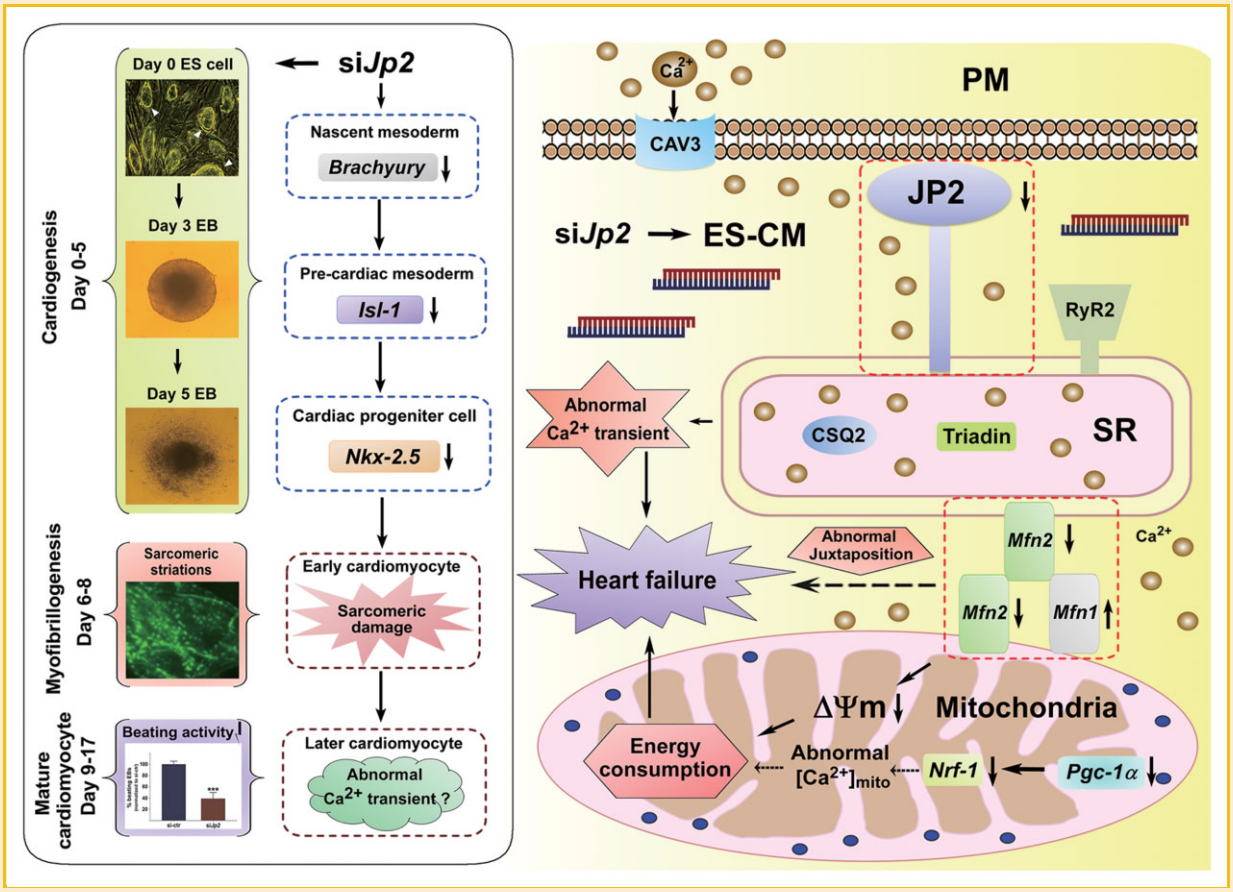

Fig. 5. A schematic diagram summarizing major findings of this study. The data demonstrated that decreasing *Jp2* by acute siRNA in ESC-CMs resulted in (i) affecting energy production (toward low ΔΨm) accompanied by impairing functional gene expression (right box). (ii) Markedly disrupting juxtaposition of the SR with mitochondrium, indicated by reduced tethering SR to mitochondrium gene *Mfn2* expression, (iii) increased *MEF2C* expression and decreased JP2 expression accompanied by increasing in cell size, and (iv) disorderly Ca^{2+} transients in spontaneously beating or non-beating ESC-CMs. While decreasing *Jp2* expression by siRNA in ES cells resulted in (i) reducing gene expression toward mesoderm and cardiogenesis, (ii) disordering or abolishing sarcomeric structures in ESC-CMs, (iii) losing JP2 co-localization with sarcomere proteins accompanied by reduced beating activity in EBs (left box). [Color figure can be seen in the online version of this article, available at http://wileyonlinelibrary.com/journal/jcb]

HL-1 cells or ventricular myocytes from α-MerCreMer-JP2 knockdown mice [Landstrom et al., 2011; van Oort et al., 2011], but different in the mode (increase incidence of spontaneous SR Ca^{2+} release [van Oort et al., 2011] or increase basal Ca^{2+} level [Landstrom et al., 2011]). Our results further demonstrated that *Jp2* knockdown affected Ca^{2+} transients of SR in ES-CMs, which might take direct responsibility for the mitochondrial dysfunction.

Furthermore, irregular intracellular Ca^{2+} signaling could interfere with Ca^{2+}-dependent enzyme system and gene expression. Our finding revealed that si*Jp2* was directly responsible for increase in cell size and *MEF-2C* transcription in ESC-CMs. *MEF-2C* was a key transcription factor for cardiac hypertrophy which integrated multiple Ca^{2+}/calmodulin-dependent signaling pathways in cardiomyocytes [Kolodziejczyk et al., 1999; Xu et al., 2006]. As was known that *Jp2* genes mutation and mitochondrial dysfunction was closely associated with cardiac hypertrophy [Dai et al., 2011], thus, reduced *MEF-2C* transcription further established the link between mitochondrial dysfunction and abnormal SR Ca^{2+} transient which caused by si*Jp2*. Its cascade reaction between *Jp2* and *MEF-2C* should be considered to explore in next research.

Based on our knowledge, this was the first time we demonstrated that decreased JP2 expression interfered with juxtaposition of mitochondrium and SR. Mitochondrial dysfunction in si*Jp2* ESC-CMs was more likely caused by Ca^{2+} homeostasis disorder in SR, accompanied by Ca^{2+} related cardiac hypertrophic gene expression. Therefore, we concluded that the deficiency of functional crosstalk between mitochondrium mitofusin and SR was partly due to abnormal Ca^{2+} transients caused by si*Jp2*. In the si*Jp2* ESC-CMs, both mitochondrial dysfunction and Ca^{2+} related abnormalities might contribute to the embryonic lethality.

Takeshima et al. [2000] had reported that genetic ablation of JP2 resulted in embryonic lethality, most likely for the absence of cardiac contractility around embryonic day 10.5. It seemed that JP2 played an important role in the heart development. We therefore further investigated the effects of si*Jp2* on the cardiogenesis from ES cells, so as to understand the developmental events and to predict and control their differentiation for the use in cardiovascular repair. We found that mesoderm gene *Brachyury* (day 0–8), pre-cardiac mesoderm gene *Isl-1* (day 2–8), and cardiac progenitor cell gene *Nkx-2.5* (day 4–8) transcription were selectively inhibited

after si*Jp2* in ES cell, followed with abnormal sarcomere formation, indicating that *Jp2* gene might control the fate of ES cell differentiation toward mesoderm differentiation and cardiac muscle formation at the early stage. Both the organization and co-localization of the sarcomeric structures with JP2 was seriously spoiled in si*Jp2* group, meanwhile, beating phenotype was markedly abnormal contrast with the negative control. It had been reported that Ca^{2+}-mediated activation of calcineurin and NF-AT3 interacted with GATA-4 to activate a discrete set of cardiogenesis genes such as *β-MHC*, indicating the importance of Ca^{2+} signal during cardiac development [Tallini et al., 2006] [Morkin, 2000]. Thus, our data demonstrated that JP2 was an essential component of the sarcomeric structures, which would be disorder for the loss of JP2; decreased JP2 expression selectively affected sarcomeric protein, indicated by abnormal sarcomere formation and reduced beating function, one of the hallmarks of congestive HF. It was concord with the result that mutant mice lacking JP2 exhibited embryonic lethality [Takeshima et al., 2000]. Therefore, it was important to highlight that *Jp2* took a key role as early as the differentiation, and the existence of sensitive time window of *Jp2* necessary in cardiac differentiation. Unfortunately, we did not evaluate the statue of mitochondrium during cardiogenesis, which could be affected by si*Jp2* and of vital importance. This should be considered to explore in next study.

In the present research, protein components (JMCs such as cav3, triadin, CSQ2, and RyR2) contributing to cellular Ca^{2+}-handling were also investigated in the process of cardiogenesis. JMCs were often useful targets for various research purposes [Fu et al., 2006], and their developmental information was especially valuable for regeneration medicine. Our data showed that the cav3 in TTs not fully mature until late differentiation period, but the expression of triadin, CSQ2, RyR2, and JP2, appeared early and increased in a time-dependent manner. JP2, together with RyR2, the protein marker for SR, and cav3, the marker for TTs, sheared the terminal cisternae assembled from at least two distinct membrane components in ESC-CMs. This finding further confirmed that JP2 played other roles during the cardiac differentiation, in addition to anchoring the SR to the TTs.

In conclusion, our finding revealed that reducing JP2 expression in ESC-CMs resulted in injured mitochondrium status partly for the abnormal cellular Ca^{2+} homeostasis; a sensitive time window of *Jp2* necessary in cardiac differentiation was found and *Jp2* controlled the cardiogenesis of ES cells in an extra non-TTs/SR anchor-dependent manner (Fig. 5). Therefore, targeting JP2 and its effective partners might represent a new therapeutic strategy for the treatment of heart disease, and the ESC-CMs showed similar characterization of JP2 in adult cardiomyocytes, further proved could be used in cell-based regenerative strategy for HF.

ACKNOWLEDGMENTS

We thank Prof. Dr. Erqing Wei for supporting Ca^{2+} transient measurement. This work was supported by National Natural Science Foundation of China (No. 30973600, No. 90813026, No. 81173135), by Ministry of Science and Technology of China (No. 2009ZX09303-004) for the Key Project (Cardio-Cerebral Vascular Branch) of Effect Evaluation in Drug Development, and Outstanding Researcher Program in Medicine & Health Foundation of Zhejiang Province (No. 2011RCA024).

REFERENCES

Behbahani H, Shabalina IG, Wiehager B, Concha H, Hultenby K, Petrovic N, Nedergaard J, Winblad B, Cowburn RF, Ankarcrona M. 2006. Differential role of Presenilin-1 and -2 on mitochondrial membrane potential and oxygen consumption in mouse embryonic fibroblasts. J Neurosci Res 84:891–902.

Boheler KR, Czyz J, Tweedie D, Yang HT, Anisimov SV, Wobus AM. 2002. Differentiation of pluripotent embryonic stem cells into cardiomyocytes. Circ Res 91:189–201.

Chen H, Detmer SA, Ewald AJ, Griffin EE, Fraser SE, Chan DC. 2003. Mitofusins Mfn1 and Mfn2 coordinately regulate mitochondrial fusion and are essential for embryonic development. J Cell Biol 160:189–200.

Dai DF, Johnson SC, Villarin JJ, Chin MT, Nieves-Cintron M, Chen T, Marcinek DJ, Dorn GW 2nd, Kang YJ, Prolla TA, Santana LF, Rabinovitch PS. 2011. Mitochondrial oxidative stress mediates angiotensin II-induced cardiac hypertrophy and Galphaq overexpression-induced heart failure. Circ Res 108:837–846.

de Brito OM, Scorrano L. 2008. Mitofusin 2 tethers endoplasmic reticulum to mitochondria. Nature 456:605–610.

de Brito OM, Scorrano L. 2009. Mitofusin-2 regulates mitochondrial and endoplasmic reticulum morphology and tethering: The role of Ras. Mitochondrion 9:222–226.

Ding L, Liang X, Zhu D, Lou Y. 2007a. Peroxisome proliferator-activated receptor alpha is involved in cardiomyocyte differentiation of murine embryonic stem cells in vitro. Cell Biol Int 31:1002–1009.

Ding L, Liang XG, Hu Y, Zhu DY, Lou YJ. 2008. Involvement of p38MAPK and reactive oxygen species in icariin-induced cardiomyocyte differentiation of murine embryonic stem cells in vitro. Stem Cells Dev 17:751–760.

Ding L, Liang XG, Lou YJ. 2007b. Time-dependence of cardiomyocyte differentiation disturbed by peroxisome proliferator-activated receptor alpha inhibitor GW6471 in murine embryonic stem cells in vitro. Acta Pharmacol Sin 28:634–642.

Ding L, Liang XG, Zhu DY, Lou YJ. 2007c. Icariin promotes expression of PGC-1alpha, PPARalpha, and NRF-1 during cardiomyocyte differentiation of murine embryonic stem cells in vitro. Acta Pharmacol Sin 28:1541–1549.

Eura Y, Ishihara N, Oka T, Mihara K. 2006. Identification of a novel protein that regulates mitochondrial fusion by modulating mitofusin (Mfn) protein function. J Cell Sci 119:4913–4925.

Fu JD, Li J, Tweedie D, Yu HM, Chen L, Wang R, Riordon DR, Brugh SA, Wang SQ, Boheler KR, Yang HT. 2006. Crucial role of the sarcoplasmic reticulum in the developmental regulation of Ca2+ transients and contraction in cardiomyocytes derived from embryonic stem cells. FASEB J 20:181–183.

Hirata Y, Brotto M, Weisleder N, Chu Y, Lin P, Zhao X, Thornton A, Komazaki S, Takeshima H, Ma J, Pan Z. 2006. Uncoupling store-operated Ca2+ entry and altered Ca2+ release from sarcoplasmic reticulum through silencing of junctophilin genes. Biophys J 90:4418–4427.

Kapur N, Banach K. 2007. Inositol-1,4,5-trisphosphate-mediated spontaneous activity in mouse embryonic stem cell-derived cardiomyocytes. J Physiol 581:1113–1127.

Kee HJ, Kook H. 2009. Kruppel-like factor 4 mediates histone deacetylase inhibitor-induced prevention of cardiac hypertrophy. J Mol Cell Cardiol 47:770–780.

Kolodziejczyk SM, Wang L, Balazsi K, DeRepentigny Y, Kothary R, Megeney LA. 1999. MEF2 is upregulated during cardiac hypertrophy and is required for normal post-natal growth of the myocardium. Curr Biol 9:1203–1206.

Landstrom AP, Kellen CA, Dixit SS, van Oort RJ, Garbino A, Weisleder N, Ma J, Wehrens XH, Ackerman MJ. 2011. Junctophilin-2 expression silencing causes cardiocyte hypertrophy and abnormal intracellular calcium-handling. Circ Heart Fail 4:214–223.

Landstrom AP, Weisleder N, Batalden KB, Bos JM, Tester DJ, Ommen SR, Wehrens XH, Claycomb WC, Ko JK, Hwang M, Pan Z, Ma J, Ackerman MJ. 2007. Mutations in JPH2-encoded junctophilin-2 associated with hypertrophic cardiomyopathy in humans. J Mol Cell Cardiol 42:1026–1035.

Li J, Stouffs M, Serrander L, Banfi B, Bettiol E, Charnay Y, Steger K, Krause KH, Jaconi ME. 2006. The NADPH oxidase NOX4 drives cardiac differentiation: Role in regulating cardiac transcription factors and MAP kinase activation. Mol Biol Cell 17:3978–3988.

Li ZJ, Wang ZZ, Zheng YZ, Xu B, Yang RC, Scadden DT, Han ZC. 2005. Kinetic expression of platelet endothelial cell adhesion molecule-1 (PECAM-1/CD31) during embryonic stem cell differentiation. J Cell Biochem 95:559–570.

Lukyanenko V, Chikando A, Lederer WJ. 2009. Mitochondria in cardiomyocyte Ca2+ signaling. Int J Biochem Cell Biol 41:1957–1971.

Matsushita Y, Furukawa T, Kasanuki H, Nishibatake M, Kurihara Y, Ikeda A, Kamatani N, Takeshima H, Matsuoka R. 2007. Mutation of junctophilin type 2 associated with hypertrophic cardiomyopathy. J Hum Genet 52:543–548.

Mercy L, Pauw A, Payen L, Tejerina S, Houbion A, Demazy C, Raes M, Renard P, Arnould T. 2005. Mitochondrial biogenesis in mtDNA-depleted cells involves a Ca2+-dependent pathway and a reduced mitochondrial protein import. FEBS J 272:5031–5055.

Metzger JM, Lin WI, Samuelson LC. 1996. Vital staining of cardiac myocytes during embryonic stem cell cardiogenesis in vitro. Circ Res 78:547–552.

Minamisawa S, Oshikawa J, Takeshima H, Hoshijima M, Wang Y, Chien KR, Ishikawa Y, Matsuoka R. 2004. Junctophilin type 2 is associated with caveolin-3 and is down-regulated in the hypertrophic and dilated cardiomyopathies. Biochem Biophys Res Commun 325:852–856.

Morkin E. 2000. Control of cardiac myosin heavy chain gene expression. Microsc Res Tech 50:522–531.

Muller M, Fleischmann BK, Selbert S, Ji GJ, Endl E, Middeler G, Muller OJ, Schlenke P, Frese S, Wobus AM, Hescheler J, Katus HA, Franz WM. 2000. Selection of ventricular-like cardiomyocytes from ES cells in vitro. FASEB J 14:2540–2548.

Parekh A. 2009. Calcium signalling: Mitofusins promote interorganellar crosstalk. Curr Biol 19:R200–R203.

Rizzuto R, Pozzan T. 2006. Microdomains of intracellular Ca2+: Molecular determinants and functional consequences. Physiol Rev 86:369–408.

Satin J, Itzhaki I, Rapoport S, Schroder EA, Izu L, Arbel G, Beyar R, Balke CW, Schiller J, Gepstein L. 2008. Calcium handling in human embryonic stem cell-derived cardiomyocytes. Stem Cell 26:1961–1972.

Shao D, Liu Y, Liu X, Zhu L, Cui Y, Cui A, Qiao A, Kong X, Chen Q, Gupta N, Fang F, Chang Y. 2010. PGC-1 beta-regulated mitochondrial biogenesis and function in myotubes is mediated by NRF-1 and ERR alpha. Mitochondrion 10:516–527.

Takeshima H. 2003. Ryanodine receptor and junctional membrane structure. Nippon Yakurigaku Zasshi 121:203–210.

Takeshima H, Komazaki S, Nishi M, Iino M, Kangawa K. 2000. Junctophilins: A novel family of junctional membrane complex proteins. Mol Cell 6:11–22.

Tallini YN, Ohkura M, Choi BR, Ji G, Imoto K, Doran R, Lee J, Plan P, Wilson J, Xin HB, Sanbe A, Gulick J, Mathai J, Robbins J, Salama G, Nakai J, Kotlikoff MI. 2006. Imaging cellular signals in the heart in vivo: Cardiac expression of the high-signal Ca2+ indicator GCaMP2. Proc Nat Acad Sci USA 103:4753–4758.

van Oort RJ, Garbino A, Wang W, Dixit SS, Landstrom AP, Gaur N, De Almeida AC, Skapura DG, Rudy Y, Burns AR, Ackerman MJ, Wehrens XH. 2011. Disrupted junctional membrane complexes and hyperactive ryanodine receptors after acute junctophilin knockdown in mice. Circulation 123:979–988.

Wallace DC. 1999. Mitochondrial diseases in man and mouse. Science 283: 1482–1488.

Wo Y, Zhu D, Yu Y, Lou Y. 2008a. Involvement of NF-kappaB and AP-1 activation in icariin promoted cardiac differentiation of mouse embryonic stem cells. Eur J Pharmacol 586:59–66.

Wo YB, Zhu DY, Hu Y, Wang ZQ, Liu J, Lou YJ. 2008b. Reactive oxygen species involved in prenylflavonoids, icariin and icaritin, initiating cardiac differentiation of mouse embryonic stem cells. J Cell Biochem 103:1536–1550.

Wobus AM, Kaomei G, Shan J, Wellner MC, Rohwedel J, Ji G, Fleischmann B, Katus HA, Hescheler J, Franz WM. 1997. Retinoic acid accelerates embryonic stem cell-derived cardiac differentiation and enhances development of ventricular cardiomyocytes. J Mol Cell Cardiol 29:1525–1539.

Woo JS, Hwang JH, Ko JK, Weisleder N, Kim do H, Ma J, Lee EH. 2010. S165F mutation of junctophilin 2 affects Ca2+ signalling in skeletal muscle. Biochem J 427:125–134.

Xu J, Gong NL, Bodi I, Aronow BJ, Backx PH, Molkentin JD. 2006. Myocyte enhancer factors 2A and 2C induce dilated cardiomyopathy in transgenic mice. J Biol Chem 281:9152–9162.

Zuliani T, Duval R, Jayat C, Schnebert S, Andre P, Dumas M, Ratinaud MH. 2003. Sensitive and reliable JC-1 and TOTO-3 double staining to assess mitochondrial transmembrane potential and plasma membrane integrity: Interest for cell death investigations. Cytometry A 54:100–108.